pK_a Values and the pH Dependent Stability of the N-Terminal Domain of L9 as Probes of Electrostatic Interactions in the Denatured State. Differentiation between Local and Nonlocal Interactions†

Brian Kuhlman,‡ Donna L. Luisi,‡ Paul Young,§ and Daniel P. Raleigh*,‡,||,

Department of Chemistry, State University of New York at Stony Brook, Stony Brook, New York 11794-3400, Department of Chemistry, York College, CUNY, Jamaica, New York 11451, and Graduate Program in Biophysics and Graduate Program in Molecular and Cellular Biology, State University of New York at Stony Brook, Stony Brook, New York 11794

Received December 14, 1998; Revised Manuscript Received February 4, 1999

ABSTRACT: pK_a values were measured for the 6 carboxylates in the N-terminal domain of L9 (NTL9) by following NMR chemical shifts as a function of pH. The contribution of each carboxylate to the pH dependent stability of NTL9 was estimated by comparing the pK_a values for the native and denatured state of the protein. A set of peptides with sequences derived from NTL9 were used to model the denatured state. In the protein fragments, the pK_a values measured for the aspartates varied between 3.8 and 4.1 and the pK_a values measured for the glutamates varied between 4.1 and 4.6. These results indicate that the local sequence can significantly influence pK_a values in the denatured state and highlight the difficulties in using standard pK_a values derived from small compounds. Calculations based on the measured pK_a values suggest that the free energy of unfolding of NTL9 should decrease by 4.4 kcal mol^{-1} when the pH is lowered from 6 to 2. In contrast, urea and thermal denaturation experiments indicate that the stability of the protein decreases by only 2.6 kcal mol^{-1} when the carboxylates are protonated. This discrepancy indicates that the protein fragments are not a complete representation of the denatured state and that nonlocal sequence effects perturb the pK_a's in the denatured state. Increasing the salt concentration from 100 to 750 mM NaCl removes the discrepancy between the stabilities derived from denaturation experiments and the stability changes calculated from the pK_a values. At high concentrations of salt there is also less variation of the pK_a values measured in the protein fragments. Our results argue that in the denatured state of NTL9 there are electrostatic interactions between groups both local and nonlocal in primary sequence.

In general, it is difficult to determine the strength of the interactions that provide stability to a protein. Mutational analysis probes the importance of particular residues but often involves changes in size, hydrophobicity, conformational flexibility and polarity. Probably the most tractable interactions to study experimentally are those involving charged amino acids. By changing the pH, the charges on the residues can be altered with only small perturbations to the system. Adding or removing a proton to a side chain has little effect on the size of the residue, and changes in pH do not have large effects on the solvation properties of water as do changes in temperature or the addition of denaturant. The pK_a of a charged group reflects its electrostatic environment. Favorable charge−charge interactions will lower the pK_a of a carboxylate while unfavorable interactions will raise the pK_a. The difference in the pK_a of a charged group between the native and denatured state indicates whether the charge stabilizes or destabilizes the protein (*1*).

If the difference in the number of protons bound to the native and denatured protein can be determined as a function of pH, then the pH dependent stability of the protein can be determined. The standard approach involves the measurement of the pK_a's of the titratable groups in the native state and the use of model compound values for the pK_a's of the denatured state. If both sets of pK_a values are known, then the change in the number of bound protons can be estimated (*2*). Studies with the proteins barley chymotrypsin inhibitor 2, barnase, and turkey ovomucoid third domain demonstrate that the most difficult part of this process is estimating the pK_a values for the denatured state (*3*−*5*). If model compound values are used to approximate the pK_a values of the denatured state, then the predicted changes in stability are larger than the observed changes. These discrepancies have been attributed to electrostatic interactions in the denatured state. Here, we examine the pH dependence of the stability of a small, mixed $\alpha-\beta$ protein, the N-terminal domain of L9. One of the goals of this study is to determine if more

† This work was supported by NSF grant MCB 9600866 to DPR. DPR is a Pew Scholar in the Biomedical Sciences. The NMR facility at SUNY Stony Brook is supported by a grant from the NSF, CHE9413510. PY was supported by a MARC senior faculty fellowship from the NIH (1F33GM18620−01). BK was supported in part by a Graduate Council Fellowship from the State University of New York.

* Corresponding author: Department of Chemistry, State University of New York at Stony Brook, Stony Brook, NY 11794-3400. Phone: 516 632-9547. Fax: 516 632-7960. E-mail: DRaleigh@ccmail.sunysb.edu.

‡ Department of Chemistry, SUNY.

§ York College, CUNY.

|| Graduate Programs in Biophysics and Molecular and Cellular Biology, SUNY.

10.1021/bi982931h CCC: $18.00
Published on Web 03/19/1999

Table 1: Peptide Fragments of NTL9 Used in This Study

fragment	sequence[a]
L9: 1−11	NH_3−MKVIFLKDVKG−NH_2
L9: 12−23	Ac−KGKKGEIKNVAD−NH_2
L9: 21−27	Ac−VADGYAN−NH_2
L9: 35−42	Ac−LAIEATPA−NH_2
L9: 40−56	Ac−TPANLKALEAQKQKEQR−NH_2

[a] NH_3 denotes a free N-terminus, NH_2 denotes an amidated C-terminus, and Ac denotes an acetylated N-terminus.

realistic models of local sequence effects in the denatured state can account for deviations between measured and calculated stabilities. To this end we have used a set of peptides derived from the N-terminal domain of L9 (NTL9)[1] to model local interactions in the denatured state (*6*). The pK_a values measured in these protein fragments should provide a better estimate of the pK_a values in the denatured state than can be obtained with simple model compounds. A second goal of this work is to probe for the presence of long range nonrandom structure in the denatured state.

The N-terminal domain of L9 (NTL9) folds reversibly via a two-state mechanism (*7, 8*) and is particularly well suited for pH dependent studies because it remains folded over the pH range of 1.5 to 12.5. It is 56 residues long and forms a three stranded β-sheet sandwiched between two helices (*9, 10*). It does not contain any disulfides or metal binding sites. There are 19 charged groups in the protein. The sequence includes 2 aspartates, 4 glutamates, 11 lysines, one arginine, and a free N-terminus.

MATERIALS AND METHODS

Sample Synthesis and Purification. The N-terminal domain of L9 from *Bacillus stearothermophilus*, residues 1−56, was prepared by chemical synthesis and purified as described previously (*7*). The C-terminus is amidated and the N-terminus is free. Peptide fragments of the N-terminal domain of L9 were prepared as described previously (*6*). Table 1 lists the sequences of the fragments that were synthesized. The N- and C-termini of the peptides were blocked with acetyl and carboxamide groups, respectively, with the exception that the peptide corresponding to residues 1−11 of L9 has a free N-terminus.

Sample Preparation. Lyophilized peptide or protein was dissolved in 10 mM sodium phosphate, 90% H_2O, 10% D_2O containing either 100 or 750 mM NaCl. NTL9 and the peptides were lyophilized from HPLC buffers containing 0.1% trifluoroacetic acid (TFA), and therefore the prepared solutions also contain small amounts of TFA, approximately 10 mM TFA for a 1 mM solution of NTL9. Freshly dissolved solutions were between pH 3 and 6.5, depending on the concentration of peptide or protein. Solutions were adjusted to the desired pH with HCl and NaOH. For the NMR samples that contain high concentrations of peptide or protein, a final concentration of 30−40 mM HCl was required to adjust the pH from 7 to 2. For the circular dichroism (CD) experiments, the addition of HCl to a final concentration of 20−30 mM HCl was used to lower the pH from 7 to 2.

[1] Abbreviations: CD, circular dichroism; GuHCl, guanidine hydrochloride; NMR, nuclear magnetic resonance; NTL9, N-terminal domain of L9; TFA, trifluoroacetic acid; TOCSY, total correlated spectroscopy; TSP, 3-(trimethylsilyl) propionate.

Urea solutions were used within one day of preparation. Urea denaturations were performed by making two solutions of identical protein concentration, one with no urea and one with high concentrations of urea, and then titrating one solution into the other. Aliquots were removed after each addition to determine the exact concentration of denaturant by refractance (*11*). In the far-UV CD studies the protein concentrations were between 10 and 20 μM, and in the near-UV CD studies the protein concentrations were between 300 and 400 μM. In the NMR studies, the concentration of NTL9 was 2 mM. In the NMR studies of the peptide fragments of NTL9, the peptide concentrations were 2−6 mM.

pH Measurements. pH measurements were made using an accumet pH meter 15 and an accumet combination electrode with a calomel reference. The pH meter was calibrated with three commercial standards pH 2, pH 4, and pH 7 (Fisher Scientific). pH values measured before and after the experiments differed by less than 0.1, and the reported pH values are an average of these two pH readings.

Protein Stability Measurements. Protein stability was measured at various pHs by chemical and thermal denaturation. Chemical denaturation was monitored with far-UV (222 nm) CD and thermal denaturation was monitored with near-UV (280 nm) CD. CD spectroscopy was performed using an Aviv 62A DS spectrometer equipped with a Peltier temperature control unit. Temperature melts were performed between 1 and 97 °C at 2 °C intervals. Ellipticity at 280 nm was averaged for 45 s at each temperature following a one minute equilibration period. An external thermocouple was used to determine the optimum equilibration time and overshoot parameters. Solutions were stirred during the temperature melt. For denaturation experiments with urea, the ellipticity at 222 nm was averaged for 60 s at various urea concentrations. Thermal denaturations were used at low pH to calculate $\Delta G°$ because there was little or no pretransition in the urea denaturations. Urea denaturations were used at high pH because determining the stability from thermal melts at high pH requires a long extrapolation to 25 °C.

The data from the urea denaturations, ellipticity versus urea concentration, were fit to eq 1 using the nonlinear least-squares regression routine in the program SigmaPlot.

$$\theta([\text{urea}]) = (\theta_N + \theta_D \exp(-\Delta G°([\text{urea}])/RT))/(1 + \exp(-\Delta G°([\text{urea}])/RT)) \quad (1)$$

where

$$\Delta G°([\text{urea}]) = \Delta G°(0\ \text{M urea}) - m[\text{urea}] \quad (2)$$

and θ_N and θ_D are given by

$$\theta_N([\text{urea}]) = a + b[\text{urea}] \quad (3)$$

$$\theta_D([\text{urea}]) = c + d[\text{urea}] \quad (4)$$

θ is the measured ellipticity, θ_N is the ellipticity of the native state, θ_D is the ellipticity of the denatured state, $\Delta G°$ is the free energy change for the unfolding reaction, T is temperature, and R is the gas constant. There a total of six adjustable parameters. The four parameters that define the ellipticity of the native and denatured states, a, b, c and d, as well as $\Delta G°$ (0 M urea) and m.

Thermal denaturations were fit with an expression of the same type as eq 1 with $\Delta G°$([urea]) replaced by $\Delta G°(T)$. $\Delta G°(T)$ is given by the Gibbs−Helmholtz expression:

$$\Delta G°(T) = (\Delta H°(T_0) - T\Delta S°(T_0)) + (\Delta C_p°(T - T_0 + T * \ln(T_0/T))) \quad (5)$$

T_0 is a reference temperature, $\Delta H°$ (T_0) is the change in enthalpy for the unfolding reaction at the reference temperature, $\Delta S°$ (T_0) is the change in entropy, and $\Delta C_p°$ is the change in heat capacity. $\Delta C_p°$ was set to the previously determined value of 0.53 kcal mol^{-1} deg^{-1} (*12*) while $\Delta H°(T_0)$ and $\Delta S°(T_0)$ were adjustable parameters. T_0 was set to 298.15 K.

Determination of pK_a's using Nuclear Magnetic Resonance (NMR). pK_a's were determined by monitoring chemical shifts as a function of pH. The chemical shifts of the C$^\beta$ protons on aspartate and the C$^\gamma$ protons on glutamate move downfield by approximately 0.2 ppm when the carboxyl group is protonated. Data were fit to the Henderson-Hasselbalch equation (eq 6) in order to determine pK_a's:

$$\delta(\mathrm{pH}) = (\delta_{base} + \delta_{acid}10^{(pK - pH)})/(1 + 10^{(pK - pH)}) \quad (6)$$

where δ is the chemical shift, δ_{base} is the chemical shift associated with the unprotonated residue, δ_{acid} is the chemical shift associated with the protonated residue, and pK is the pK_a value for the residue. Data were fit using the nonlinear least-squares regression routine in the program SigmaPlot. Data were also fit to a Hill equation that assumes that there are n protons titrating simultaneously at each position:

$$\delta(\mathrm{pH}) = (\delta_{base} + \delta_{acid}10^{n(pK - pH)})/(1 + 10^{n(pK - pH)}) \quad (7)$$

NMR experiments were performed on Varian Instrument's Inova 500 and 600 MHz spectrometers. All spectra were internally referenced to TSP. Chemical shift data were corrected for the pH dependence of the TSP chemical shift using eq 8.

$$\delta_{corr} = (\delta_{obs} - 0.019)(1 + 10^{(5-pH)})^{-1} \quad (8)$$

TOCSY experiments with 75 ms mixing times were performed at various pHs in order to determine the chemical shifts as a function of pH. The peaks in the 2D NMR spectra were identified using previously determined assignments at pH 5.0 (*6*, *7*).

Error Analysis. Uncertainties in $\Delta G°$ (0 M urea, 25 °C) were obtained by perturbing $\Delta G°$ (0 M urea, 25 °C) from its best fit value and then observing how this change affects the chi-squared value for a new fit. The parameters not being analyzed are allowed to change. An F test was then performed to determine what chi-squared value corresponds to the 95% confidence limit. The error for the parameter is then determined by the range of $\Delta G°$ (0 M urea, 25 °C) values that give chi-squared values lower than the maximum allowed chi-squared determined by the F test. The errors are not necessarily symmetrical around the best fit value. This statistical procedure is described in more detail in Shoemaker et al. (*13*). When determining the error for $\Delta G°$ (0 M urea, 25 °C) obtained from a temperature melt, eq 5 was rewritten so that $\Delta G°$ (0 M urea, 25 °C) was one of the fitted parameters. Estimates of the limits of error in pK_a values and Hill coefficients were obtained using the standard error values given by SigmaPlot and the appropriate Student t-values (*13*).

Activity Coefficients. The activity coefficient for a carboxylate as a function of ionic strength was estimated using the extended Debye−Hückel law (*14*):

$$\log \gamma = -Az^2 \frac{\sqrt{I}}{1 + Ba\sqrt{I}} \quad (9)$$

where γ is the activity coefficient, $A = 0.509$ mol$^{-1/2}$ kg$^{1/2}$ at 25 °C, z = the charge on the ion, I is ionic strength, and $B = 0.328$ mol$^{-1/2}$ kg$^{1/2}$ at 25 °C. The adjustable parameter, a, corresponds roughly to the effective size of the hydrated ion (*14*). It was set to 4 which is the parameterized value for CH_3COO^-. Equation 9 predicts that $\log(\gamma) = -0.11$ at $I = 0.1$ and -0.21 at $I = 0.75$. The activity coefficient was also estimated using the Davies equation (*14*). The Davies equation predicts that $\log(\gamma) = -0.11$ at $I = 0.1$ and -0.16 at $I = 0.75$.

RESULTS

Stability Measurements. The stability of NTL9 was measured between pH 7 and pH 2 at moderate (100 mM NaCl) and high (750 mM NaCl) salt. The stabilities were measured using thermal and chemical denaturation experiments (Figure 1). The results from these experiments are shown in Table 2 which lists the values of $\Delta G°$ of unfolding determined at different pHs. NTL9 is more stable at neutral pH but remains folded below pH 2. The 1D NMR spectrum recorded at low pD is essentially identical to the 1D NMR spectrum recorded at neutral pD, indicating that there are no significant structural perturbations in the protein when the pH is changed between 7 and 2. The addition of salt stabilizes NTL9 at all pHs examined. At pH 7.0 the stability of NTL9 is 4.5 (+1.5, −0.9) kcal mol^{-1} in 100 mM NaCl, while in 750 mM NaCl the stability is 5.2 (+1.3, 0.9) kcal mol^{-1} at pH 7.3. At pH 2.0 the stability is 1.9 (+0.6, −0.5) kcal mol^{-1} in 100 mM NaCl, while in 750 mM NaCl the stability is 2.9 (+0.5, −0.5) at pH 2.4. The numbers in parentheses represent the range of the 95% confidence limits.

pK_a Values for the Native State of NTL9. There are six acidic groups in NTL9: Asp 8, Glu 17, Asp 23, Glu 38, Glu 48, and Glu 54. The location of these groups is shown in Figure 2. The C-terminus of NTL9 is amidated, and there are no histidines in the protein. The complete primary sequence is:

1	10	20
MKVIFLKDV	KGKGKKGEIK	NVADGYANNF
30	40	50
LFKQGLAIEA	TPANLKALEA	QKQKEQR

NTL9 remains folded between pH 7 and pH 2, and therefore it is possible to follow the NMR chemical shifts of these residues in the native protein as a function of pH. Of particular interest are the chemical shifts of the C$^\beta$ protons on the aspartic acid residues and the C$^\gamma$ protons on the glutamic acid residues. The chemical shifts of these protons shift downfield by approximately 0.2 ppm when the carboxyl groups on the aspartates and glutamates are protonated at low pH, and the pK_a's of the aspartates and glutamates can

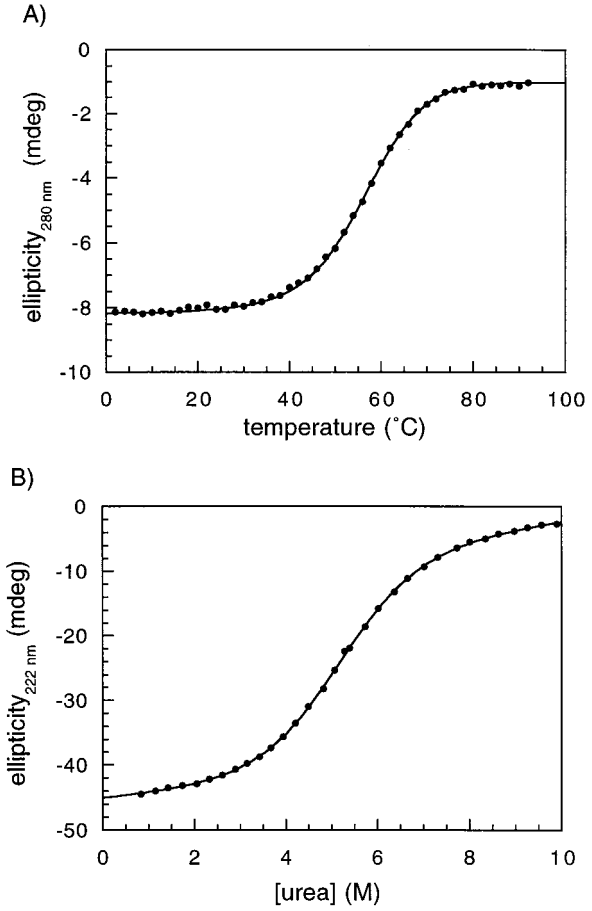

FIGURE 1: (a) Thermal and (b) chemical denaturation of NTL9 as followed by CD. The experimental data were fit with eq 1 in order to determine $\Delta G°$ (0 M urea, 25 °C). The results are listed in Table 2. The thermal denaturation was performed at pH 2.79 and the urea denaturation at pH 4.51. The solutions contained 100 mM NaCl, 10 mM sodium phosphate in 90% H_2O/10% D_2O.

Table 2: The Free Energy of Denaturation of NTL9 as a Function of pH[a]

(100 mM NaCl)		(750 mM NaCl)	
pH (of measurement)	$\Delta G°$ (kcal mol^{-1})	pH of measurement	$\Delta G°$ (kcal mol^{-1})
2.04	1.9 (+0.6, −0.5)[b,d]	2.40	2.9 (±0.5)[c]
2.79	2.3 (+0.5, −0.4)[b]	3.15	3.1 (±0.5)[c]
3.55	3.0 (+0.8, −0.6)[b]	4.14	4.0 (+0.9, −0.7)[c]
4.51	3.5 (±0.5)[c]	5.25	4.8 (+1.0, −0.8)[c]
5.99	4.4 (+0.6, −0.5)[c]	6.56	4.7 (+0.8, −0.6)[c]
6.98	4.5 (+1.5, −0.9)[c]	7.26	5.2 (+1.3, −0.9)[c]

[a] Experiments were performed in 10 mM sodium phosphate with either 100 mM or 750 mM NaCl at 25 °C in 90% H_2O, 10% D_2O. [b] $\Delta G°$ was determined from a thermal denaturation of NTL9. [c] $\Delta G°$ was determined from an urea denaturation of NTL9. [d] Errors represent 95% confidence limits and were determined as described in Materials and Methods.

be determined by monitoring the chemical shifts as a function of pH. The pK_a's were determined for all six residues by fitting the data to the Henderson−Hasselbalch equation (Figures 3 and 4). The results are listed in Table 3.

pK_a values are indicative of the environment of a charged group. If an aspartate or glutamate is involved in a favorable interaction such as a salt bridge or a hydrogen bond, then it will be more difficult to protonate and the residue will have a lower pK_a. If the charged group is in an unfavorable

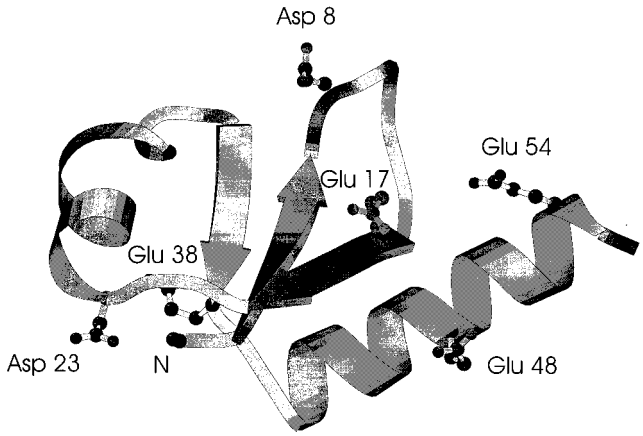

FIGURE 2: Molscript (*30*) diagram of NTL9. The positions of the aspartic acid and glutamic acid residues are shown as is the location of the N-terminus.

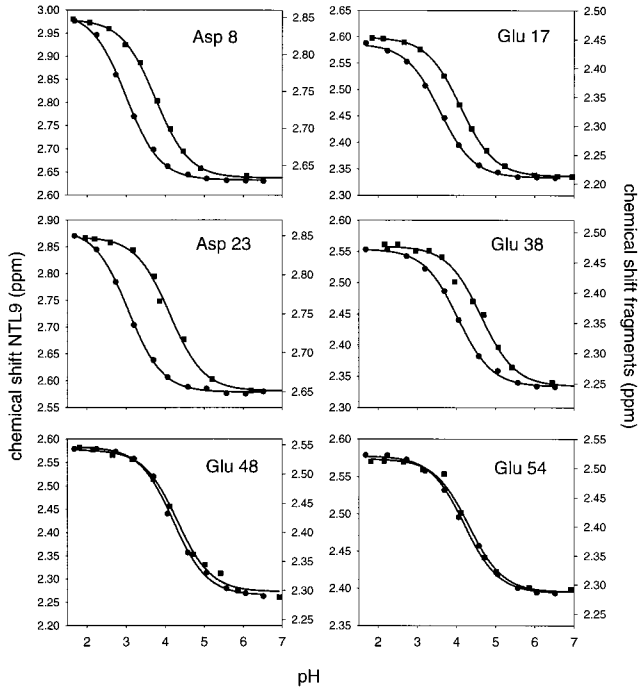

FIGURE 3: Chemical shift as a function of pH in 100 mM NaCl for NTL9 (circles) and the peptide fragments of NTL9 (squares). The left axis reports the chemical shifts for NTL9 and the right axis reports the chemical shifts for the fragments. The C^β protons are plotted for the aspartates and the C^γ protons are plotted for the glutamates. The data were fit with the Henderson−Hasselbalch equation (eq 7) in order to determine pK_a's. The results are listed in Table 3. The solutions contained 100 mM NaCl, 10 mM sodium phosphate in 90% H_2O/10% D_2O. The temperature was 25 °C.

interaction, then it will be easier to protonate and will have a higher pK_a. In model compounds, aspartates typically have a pK_a around 3.9−4.0 and glutamates typically have a pK_a between 4.3 and 4.5. In NTL9, Asp 8, Glu 17, and Asp 23 have pK_a's that are significantly below these values, indicating that they are involved in favorable electrostatic interactions that are not present in the model compounds.

The perturbed pK_a values for Asp 8, Glu 17, and Asp 23 can be rationalized by examining the structure of NTL9. Asp 23 has a pK_a of 3.05 in NTL9. The carboxylate oxygens are located within 3 Å of the positively charged amino group at the N-terminus of the protein (Figure 2). Glu 17 has a pK_a of 3.57 and the carboxylate oxygens form a hydrogen bond

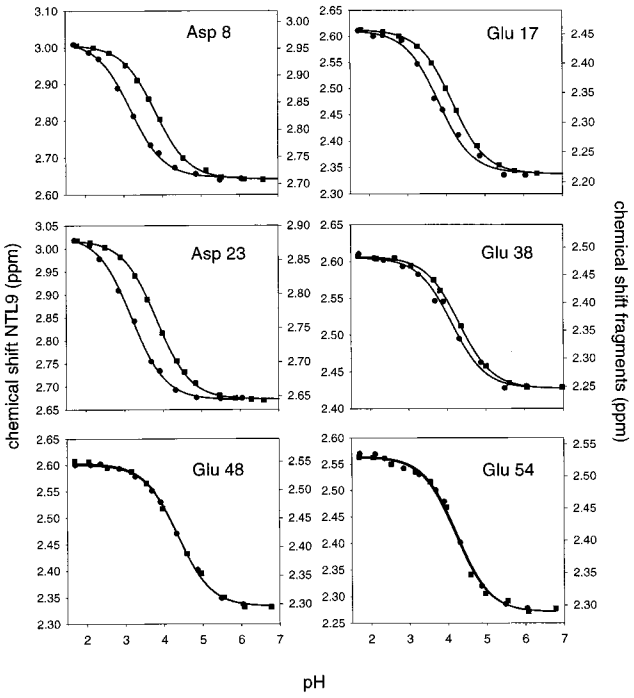

FIGURE 4: Chemical shift as a function of pH in 750 mM NaCl for NTL9 (circles) and the peptide fragments of NTL9 (squares). The left axis reports the chemical shifts for NTL9 and the right axis reports the chemical shifts for the fragments. C^{β} proton chemical shifts are plotted for the aspartates and C^{γ} proton chemical shifts are plotted for the glutamates. The data were fit with the Henderson-Hasselbalch equation (eq 7) in order to determine pK_a's. The results are in Table 3. The solutions contained 750 mM NaCl, 10 mM sodium phosphate in 90% H_2O/10% D_2O. The temperature was 25 °C.

with the backbone amide of Lys 14. Strong evidence for this hydrogen bond derives from an examination of the chemical shift of the amide proton of Lys 14 as a function pH. As Glu 17 is protonated, the amide chemical shift of Lys 14 shifts upfield by 1.5 ppm and the apparent pK_a of the transition, 3.58, is the same as the pK_a of Glu 17 (Figure 5). Similar perturbations in chemical shift have been seen in other systems in which there is a hydrogen bond between an amide and a carboxylate (*15*). There is a medium range NOE between one of the β-protons on Glu 17 and the amide proton on Lys 14 (*7*) that is also consistent with the formation of a hydrogen bond between Lys 14 and Glu 17. Asp 8 has a pK_a of 2.99. In the structure of NTL9, Asp 8 is located at the start of a lysine-rich loop that connects β-strand 1 with β-strand 2. There are 5 lysines in the loop.

The pK_a's of Glu 38, Glu 48, and Glu 54 are not significantly perturbed from model compound values. Glu 38 is largely solvent exposed and is not near (the closest charged group is the amino group on Lys 32, 7 Å) any charged groups in the structure. Glu 48 and Glu 54 are located in the C-terminal helix of NTL9 and are exposed to solvent. There are lysines located at positions 45 and 51 that may potentially form salt bridges with the glutamates. Because the pK_a's are not perturbed, it appears that these potential salt bridges either do not form, or if they do, they do not have a large effect on protein stability. Similar results have been noticed for other potential salt bridges located on the surface of proteins (*16, 17*). Yang and Honig describe three reasons why salt bridges on the surfaces of proteins do not generally make significant contributions to the net stability (*18*): (1) Charge−charge interactions on the surface of a protein are screened by the high dielectric constant of water, (2) the desolvation penalty for forming a salt bridge is high, and (3) there is an entropic penalty for fixing the side chains in the appropriate positions to form a salt bridge. The last factor may explain why the salt bridge between Asp 23 and the N-terminus is favorable and the potential salt bridges in the helix are not. In both cases the residues are solvent exposed, but in the case of Asp 23 and the N-terminus the positions of the charged groups are more fixed. The side chain of Met 1 forms part of the hydrophobic core of NTL9 and fixes the location of the N-terminal amino group. Also, an aspartic acid has fewer degrees of freedom than a glutamic acid. Therefore, there may be a smaller entropic penalty for forming the salt bridge between Asp 23 and the N-terminus.

In 750 mM NaCl, the pK_a values for NTL9 move closer to model compound values (Table 3). Similar changes have been observed in studies with other proteins (*3, 19*). It is thought that the increase in ionic strength reduces the attractive interactions between the carboxylates and the neighboring positive ions/partial charges.

The pK_a values were determined by fitting the data to the Henderson−Hasselbalch equation. This expression is only strictly valid for a single charge titrating in a constant environment. In the case of NTL9, there are six carboxylates titrating and the removal of a charge from one carboxylate may perturb the ionization state of a neighboring carboxylate. To probe for the presence of these sorts of interactions, the data were also fit with a modified Hill equation (eq 7). If the titration curve of a residue is broadened by the titration of other residues then it will have a Hill coefficient (n) below 1, and if the titration is sharper than expected for an isolated group, the Hill coefficient will be greater than 1. The net charge on NTL9 varies between +7 and +13 as the pH is lowered from 7 to below 2, and it is expected that as the net charge on the protein increases it will be more difficult to protonate the carboxylates (Hill coefficient < 1). The Hill coefficients for NTL9 are listed in Table 4. They are all near 1 within error but do have an average value, 0.95, below 1. The Hill coefficients indicate that there are no strong cooperative effects between the carboxylates, which is reasonable given that the carboxylates are not located near each other in the structure of NTL9. The closest pair is Asp 8 and Glu 17 which are 9.5 Å apart. The pK_a's determined with the modified Hill equation, eq 7, are all within 0.02 units of the pK_a's determined with the unmodified Henderson−Hasselbalch equation, eq 6.

pK_a Values for Peptide Fragments of NTL9. If the pK_a values are known for the native and denatured state of a protein, then it is possible to estimate the pH dependent stability of the protein. The following linkage relationship applies to this situation (*2*):

$$\frac{\partial \Delta G^{\circ}}{\partial \mathrm{pH}} = (2.303)RT\Delta Q \qquad (10)$$

where ΔG° is the change in free energy for the unfolding reaction, R is the gas constant, T is the temperature in Kelvin, and ΔQ is the difference in the number of charged groups between the denatured state and the native state (denatured − native). ΔQ can be estimated if the pK_a values of the native and denatured state are known. Measuring the pK_a's for the

Table 3: pK_a Values for the Acidic Residues in NTL9 and in Protein Fragments of NTL9[a]

	pK_a^{NTL9}		p$K_a^{fragment}$		
residue	100 mM NaCl	750 mM NaCl	100 mM NaCl	750 mM NaCl	fragment
Asp 8	2.99 ± 0.05	3.17 ± 0.07	3.84 ± 0.06	3.82 ± 0.03	1−11
Glu 17	3.57 ± 0.05	3.80 ± 0.12	4.11 ± 0.17	4.15 ± 0.02	12−23
Asp 23	3.05 ± 0.04	3.18 ± 0.05	4.11 ± 0.11	3.83 ± 0.01	21−27
Glu 38	4.04 ± 0.05	4.12 ± 0.14	4.63 ± 0.14	4.30 ± 0.04	35−42
Glu 48	4.21 ± 0.08	4.35 ± 0.05	4.31 ± 0.12	4.35 ± 0.08	40−56
Glu 54	4.21 ± 0.08	4.23 ± 0.09	4.32 ± 0.14	4.19 ± 0.11	40−56

[a] Solutions contained 10 mM sodium phosphate in 90% H_2O, 10% D_2O at 25 °C with either 100 mM or 750 mM NaCl. The pK_a values were obtained by fitting the data to eq 7. The C^β protons were used to determine the pK_a values for aspartates and the C^γ protons were used for the glutamates. Errors represent 95% confidence limits and were obtained as described in Materials and Methods.

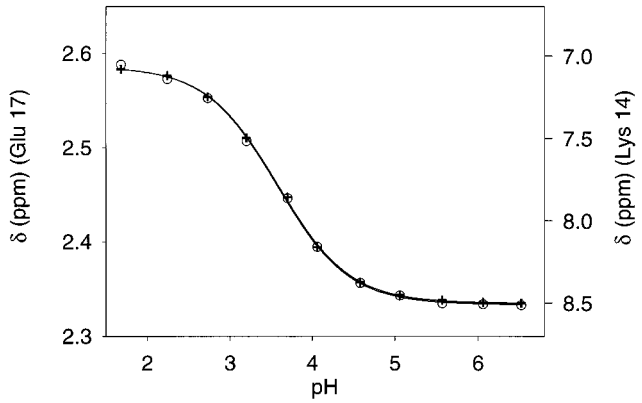

FIGURE 5: Chemical shift as a function of pH for a C^γ proton on Glu 17 (circles) and the NH proton (squares) on Lys 14. The left axis reports the chemical shift for the C^γ proton and the right axis reports the chemical shift for the NH group. Both groups titrate with the same pK_a. The solutions contained 100 mM NaCl, 10 mM sodium phosphate in 90% H_2O/10% D_2O. The temperature was 25 °C.

native state is relatively straightforward as demonstrated in the previous section. Measuring the pK_a's for the denatured state is more difficult. The denatured state is not stable under physiological conditions, and therefore model compounds need to be used. Simple peptide models that contain the charged group of interest can be used but may not be the most appropriate. A better model may be peptide fragments of the protein sequence (*20*). These peptides will model the local sequence effects that are likely to be present in the denatured state. In this study we use five different peptides to model the denatured state of NTL9 (Table 1). All of the peptides are monomeric, and all but one are predominantly unstructured as evidenced by NMR studies and CD measurements (*6*). The fragment that is derived from the C-terminal helix of NTL9, residues 40−56, is 40% helical at room temperature. It is assumed that this helicity is maintained in the denatured state of NTL9.

The pK_a values for the acidic groups in the different peptides are listed in Table 3. One striking result is that residues of a particular type do not necessarily have the same pK_a value. Asp 8 has a pK_a value of 3.84 and Asp 23 has a pK_a value of 4.11. Glu 38 has a pK_a value of 4.63 while the other glutamates have pK_a's between 4.11 and 4.32. Residues Glu 48 and Glu 54 are both located in the helical fragment and could potentially form salt bridges with Lys 45 and Lys 51. However, the pK_a's of both Glu 48 and Glu 54 are not significantly perturbed, suggesting that salt bridges involving these residues do not play a major role in stabilizing the helical structure. The pK_a of Lys 45 and Lys 51 are also not significantly perturbed (6), further supporting this conclusion. The interactions which stabilize this peptide have been analyzed in detail as part of a study of the conformational tendencies of peptide fragments of NTL9 (6). The pK_a values appear to correlate with the presence or absence of additional charged groups in the peptides. Asp 8 is in the L9: 1−11 peptide which contains 4 groups with a positive charge, while Asp 23 is the only charge group in L9: 21−27. Glu 38 is in a fragment, L9: 35−42, with no other charges, while the other glutamates are in fragments which contain several positively charged residues. These results indicate that local structure and sequence can have an appreciable effect on pK_a's and highlight the difficulty in applying standard model pK_a values to the denatured state.

As the salt concentration is increased from 100 to 750 mM NaCl, the pK_a's in the peptide fragments coalesce toward common values. Asp 8 and Asp 23 now have pK_a's that are virtually identical, and the glutamate pK_a's only vary between 4.15 and 4.35. It appears that the high salt concentrations are weakening the local sequence effects on pK_a's.

The pK_a values of Asp 23 and Glu 38 decrease by approximately 0.3 units with the addition of salt, and both of these residues are in fragments that do not contain other charged groups. The apparent pK_a for a weak acid is directly

Table 4: Hill Coefficients for the Acidic Residues in NTL9 and in Protein Fragments of NTL9[a]

	n_H^{NTL9}		$n_H^{fragment}$		
residue	100 mM NaCl	750 mM NaCl	100 mM NaCl	750 mM NaCl	fragment
Asp 8	0.94 ± 0.09	0.88 ± 0.09	0.97 ± 0.08	0.95 ± 0.05	1−11
Glu 17	0.93 ± 0.08	0.87 ± 0.22	0.96 ± 0.02	0.95 ± 0.02	12−23
Asp 23	0.98 ± 0.07	0.96 ± 0.12	0.93 ± 0.25	0.94 ± 0.02	21−27
Glu 38	0.95 ± 0.09	0.83 ± 0.23	0.86 ± 0.20	0.98 ± 0.07	35−42
Glu 48	1.02 ± 0.16	0.92 ± 0.07	0.85 ± 0.16	0.87 ± 0.09	40−56
Glu 54	0.85 ± 0.10	1.02 ± 0.21	1.22 ± 0.25	1.20 ± 0.19	40−56

[a] Solutions contained either 100 mM NaCl or 750 mM NaCl in 10 mM sodium phosphate in 90% H_2O, 10% D_2O. The Hill coefficients were obtained by fitting the data to eq 8. The C^β protons were used to determine the pK_a values for aspartates and the C^γ protons were used for the glutamates. Errors represent 95% confidence limits and were obtained as described in Materials and Methods.

related to the activity coefficients (γ) of the acid (HA) and the conjugate base (A^-) by the following expression:

$$\mathrm{p}K_a\ (\text{apparent}) = \mathrm{p}K_a\ (0\ \text{ionic strength}) + \log(\gamma_{A^-}) - \log(\gamma_{HA}) \quad (11)$$

It is often possible to predict how the apparent pK_a of model compounds will change with ionic strength by setting γ_{HA} to 1 and calculating γ_{A^-} with either the extended Debye−Hückel theory or some adaptation of it that has been parameterized for high concentrations of salt. Using the extended Debye−Hückel law (see Materials and Methods) to calculate the activity coefficients at 100 and 750 mM NaCl, the predicted decrease in pK_a for Asp 23 and Glu 38 is 0.1. Using the Davies equation parameterized for high salt concentrations, the predicted decrease in pK_a is 0.05. The difference between the calculated ΔpK_a and the measured ΔpK_a may be due to several factors. The extended Debye−Hückel law and the Davies equation start to break down at high salt concentrations (*14*). At high concentrations of salt γ_{HA} will deviate from one as groups are salted in or out. On the basis of the Hofmeister series, these effects should be small for NaCl (*21*). γ_{HA} may also be influenced by interactions with other groups in the peptide. The carboxylates may be interacting with partially charged groups in the peptides, and these interactions should vary with ionic strength. Despite all of these factors, it is expected that γ_{A^-} will decrease for Asp 23 and Glu 38 as salt is added because higher concentrations of salt will stabilize the ionized form of the group. It is therefore reasonable that the pK_a's of these two groups decrease at higher ionic strength.

pK_a Values and the pH Dependent Stability of NTL9. The pH dependent stability of NTL9 can be calculated by integrating eq 10 and inputting the pK_a values for the native and denatured state into the resulting expression:

$$\Delta\Delta G°(\mathrm{pH} - \mathrm{pH}\ 6) = RT \sum_{i=1}^{j} \ln\left[\frac{(1 + 10^{(\mathrm{pH}-\mathrm{pK}_i^{N})})(1 + 10^{(6-\mathrm{pK}_i^{D})})}{(1 + 10^{(6-\mathrm{pK}_i^{N})})(1 + 10^{(\mathrm{pH}-\mathrm{pK}_i^{D})})}\right] \quad (12)$$

where *i* identifies the residue, *j* is the number of glutamates and aspartates in the protein, *R* is the gas constant, *T* is temperature in Kelvin, pK_i^N is the pK_a value for the *i*th group in the native state and pK_i^D is the pK_a value for the *i*th group in the denatured state. The results of this calculation are compared to the measured changes in stability in Figure 6. It is important to note that $\Delta G°$ is defined as $\Delta G°$ unfolding, thus the negative values of $\Delta\Delta$G° observed at low pH indicate that the folded state is less stable at low pH. In 100 mM NaCl there is a clear discrepancy between the changes in stability predicted from the measured pK_a's and the actual changes in stability. The experimental measurements and the theoretical calculations both indicate that the native state is less stable at low pH; however, the calculations overestimate the decrease in stability. The protein is 1.8 kcal mol^{-1} more stable at low pH than is predicted using eq 12. Because the pK_a values for the native state are directly measured, the discrepancy is likely due to interactions in the denatured state which shift the pK_a values from the values measured in the peptides. If, as is highly unlikely, each ionizable group were to experience the same pK_a shift, then the discrepancy amounts to an additional shift of 0.24 pK_a units for each acidic residue. The peptides that we have used to model the denatured state include local sequence effects, but they obviously cannot mimic any longer range interactions that may exist in the denatured state.

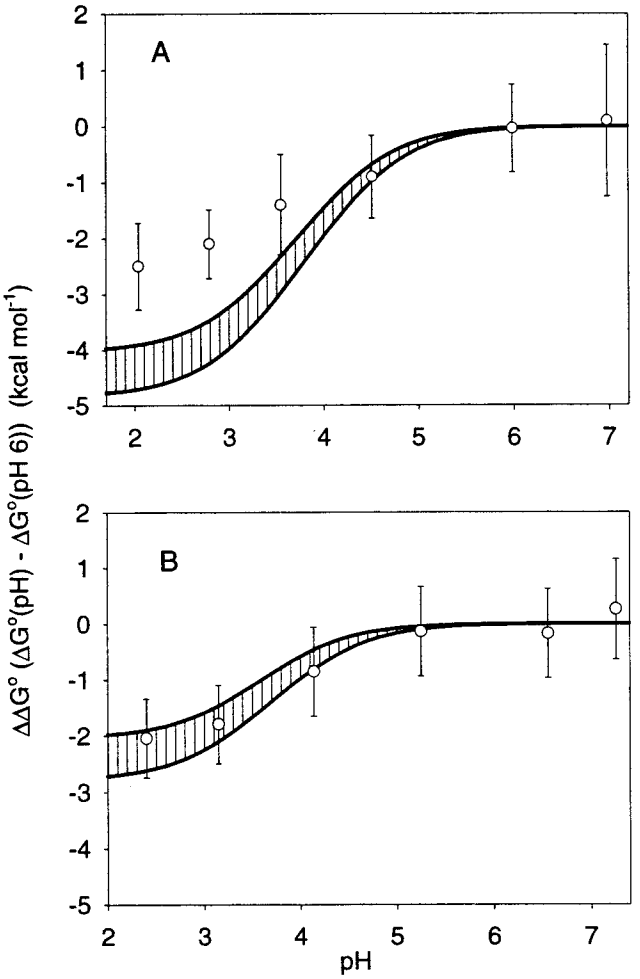

FIGURE 6: pH dependent changes in protein stability referenced to pH 6 in (a) 100 mM NaCl and (b) 750 mM NaCl. $\Delta G°$ is the free energy of unfolding. The circles are derived from chemical or thermal denaturation experiments (Table 2), and the curves are calculated using the pK_a values listed in Table 3 and eq 12. The hatched area indicates the 95% confidence limits for the calculation. The limits were determined by propagating the errors in pK_a values (Table 3) through eq 12.

In 750 mM NaCl there is good agreement between the measured changes in stability and the calculations based on the pK_a values (Figure 6). This is entirely reasonable. The pK_a values in the peptide fragments coalesce toward a single value at higher concentrations of NaCl, indicating that local sequence effects are screened at high salt. Long-range interactions are also expected to be screened at high salt.

Equation 12 is based on the Henderson−Hasselbalch equation and assumes no cooperative effects between charges. Equation 12 can be rewritten using the modified Hill equation (eq 7):

$$\Delta\Delta G°(\mathrm{pH} - \mathrm{pH}\ 6) = RT \sum_{i=1}^{j} \ln\left[\frac{(1 + 10^{n_i^{N}(\mathrm{pH}-\mathrm{pK}_i^{N})})^{(1/n_i^{N})}(1 + 10^{n_i^{D}(6-\mathrm{pK}_i^{D})})^{(1/n_i^{D})}}{(1 + 10^{n_i^{N}(6-\mathrm{pK}_i^{N})})^{(1/n_i^{N})}(1 + 10^{n_i^{D}(\mathrm{pH}-\mathrm{pK}_i^{D})})^{(1/n_i^{D})}}\right] \quad (13)$$

where n_i^N is the Hill coefficient for the *i*th group in the native state (note n_i^N is not n_i raised to the *N*th power) and n_i^D is the Hill coefficient for the *i*th group in the denatured state. Using the measured Hill coefficients (Table 4) and the pK_a values determined using eq 7, $\Delta\Delta G°$ (pH − pH 6) was calculated with eq 13. The results are nearly identical to those obtained using eq 12. The variation in $\Delta\Delta G°$ (pH − pH 6) is less than 0.04 kcal mol^{-1} at all pH values.

DISCUSSION

Our results suggest that interactions between residues that are close in primary sequence and interactions between residues more distant in primary sequence are both determinants of the pK_a's of side chains in the denatured state. The pK_a values in the different protein fragments vary significantly depending on the local sequence, demonstrating that pK_a values measured with simple model compounds will not accurately represent the values in the denatured state. The discrepancy between the measured pH dependent stability of NTL9 and that calculated from the pK_a values indicates that the pK_a values measured in the protein fragments also do not accurately represent the values in the denatured state. This provides excellent indirect evidence that there is nonrandom structure in the denatured state of NTL9. In the denatured state there may be transiently formed structure that bring charges distant in primary sequence together, and there may also be structure that influences the interactions between charges that are close in primary sequence.

In apparent contrast to our results with NTL9, the titration curve for hen egg-white lysozyme denatured in 6 M GuHCl is consistent with model compound pK_a values (*22*). One important difference between the studies is that the lysozyme studies were performed using GuHCl as a denaturant. GuHCl raises the ionic strength of the solution, and our results indicate that this will weaken both the local and nonlocal sequence effects on pK_a's in the denatured state. The strength of the denaturing conditions may also influence electrostatic interactions in the denatured state. The conformation of the denatured state in native-like conditions has more structure than proteins in 6 M GuHCl or 8 M urea (*23*). However, hydrophobic clustering has been observed in 7 M urea (*24*).

Our results are consistent with other studies that have found significant structure in the denatured state of proteins (*23*). Small-angle X-ray scattering has shown in several cases that denatured proteins often remain more compact than is predicted for a random coil (*25*−*27*). Paramagnetic relaxation studies with a spin labeled truncation mutant of staphylococcal nuclease indicate that under native conditions the denatured state has a global topology that is similar to the topology of the native state (*28*). NMR studies and fluorescence energy transfer experiments demonstrate that reduced bovine pancreatic trypsin inhibitor (BPTI) has significant structure. Electrostatic interactions in the form of charge-stabilized side chain hydrogen bonds and salt bridges were observed in molecular dynamic simulations of reduced BPTI (*29*). Interactions of this nature may be one factor contributing to the perturbed pK_a's observed in our study.

ACKNOWLEDGMENT

We thank Dr. Fernando Raineri for helpful discussions regarding the ionic strength dependence of activity coefficients.

REFERENCES

1. Anderson, D. E., Becktel, W. J., and Dahlquist, F. W. (1990) *Biochemistry 29*, 2403−2408.
2. Tanford, C. (1970) *Adv. Protein Chem. 24*, 1−95.
3. Tan, Y.-J., Oliveberg, M., Davis, B., and Fersht, A. R. (1995) *J. Mol. Biol. 254*, 980−992.
4. Swint-Kruse, L., and Robertson, A. D. (1995) *Biochemistry 34*, 4724−4732.
5. Oliveberg, M., Arcus, V. and Fersht, A. R. (1995) *Biochemistry 34*, 9424−9433.
6. Luisi, D. L., Wu, W.-J., and Raleigh, D. P. (1998) *J. Mol. Biol.*, in press.
7. Kuhlman, B., Boice, J. A., Fairman, R., and Raleigh, D. P. (1998) *Biochemistry 37*, 1025−1032.
8. Kuhlman, B., Luisi, D. L., Evans, P. A., and Raleigh, D. P. (1998) *J. Mol. Biol. 284*, 1661−1670.
9. Hoffman, D. W., Davies, C., Gerchman, S. E., Kycia, J. H., Porter, S. J., White, S. W., and Ramakrishnan, V. (1994) *EMBO J. 13*, 205−212.
10. Hoffman, D. W., Cameron, C. S., Davies, C., White, S. W., and Ramakrishnan, V. (1996) *J. Mol. Biol. 264*, 1058−1071.
11. Bower, V. E., and Robinson, R. A. (1963) *J. Phys. Chem. 67*, 1524−1527.
12. Kuhlman, B., and Raleigh, D. P. (1998) *Protein Sci. 7*, 2405−2412.
13. Shoemaker, D. P., Garland, C. W., and Nibler, J. W. (1989) *Experiments in Physical Chemistry*, 5th ed., McGraw-Hill Inc., New York.
14. Butler, J. N. (1964) *Ionic Equilibrium*, Addison-Wesley, Reading, MA.
15. Bundi, A., and Wüthrich, K. (1979) *Biopolymers 18*, 285−297.
16. Sali, D., Bycroft, M., and Fersht, A. R. (1991) *J. Mol. Biol. 220*, 779−788.
17. Dao-Pin, S., Sauer, U., Nicholson, H., and Matthews, B. W. (1991) *Biochemistry 30*, 7142−7153.
18. Yang, A.-S., and Honig, B. (1992) *Curr. Opin. Struct. Biol. 2*, 40−45.
19. Abe, Y., Ueda, T., Iwashita, H., Hashimoto, Y., and Motoshima, H. (1995) *J. Biochem. 118*, 946−952.
20. Lumb, K. J., and Kim, P. S. (1995) *Science 268*, 436−439.
21. Creighton, T. E. (1993) *Proteins*, 2nd ed., W. H. Freeman and Company, New York.
22. Roxby, R., and Tanford, C. (1971) *Biochemistry 10*, 3348−3352.
23. Shortle, D. (1996) *FASEB J. 10*, 27−34.
24. Neri, D., Billeter, M., Wider, G., and Wuthrich, K. (1992) *Science 257*, 1559.
25. Flanagan, J. A., Kataoka, M., Fujisawa, T., and Engelman, D. M. (1993) *Biochemistry 32*, 10359−10370.
26. Kataoka, M., Hagihara, Y., Mihara, K., and Goto, Y. (1993) *J. Mol. Biol. 229*, 591−596.
27. Sosnick, T. R., and Trewhella, J. (1992) *Biochemistry 31*, 8329−8335.
28. Gillespie, J. R., and Shortle, D. (1997) *J. Mol. Biol. 268*, 170−184.
29. Kazmirski, S. L., and Daggett, V. (1998) *J. Mol. Biol. 277*, 487−506.
30. Kraulis, P. J. (1991) *J. Appl. Crystallogr. 24*, 946−950.

BI982931H